

# Regucalcin confers resistance to amyloid- $\beta$ toxicity in neuronally differentiated PC12 cells

Tomiyasu Murata<sup>1</sup>, Masayoshi Yamaguchi<sup>2</sup>, Susumu Kohno<sup>3</sup>, Chiaki Takahashi<sup>3</sup>, Mitsumi Kakimoto<sup>1</sup>, Yukiko Sugimura<sup>1</sup>, Mako Kamihara<sup>1</sup>, Kiyomi Hikita<sup>1</sup> and Norio Kaneda<sup>1</sup>

1 Laboratory of Analytical Neurobiology, Faculty of Pharmacy, Meijo University, Nagoya, Japan

2 Department of Pathology and Laboratory Medicine, David Geffen School of Medicine, University of California, Los Angeles (UCLA), CA, USA

3 Division of Oncology and Molecular Biology, Cancer Research Institute, Kanazawa University, Ishikawa, Japan

## Keywords

Alzheimer's disease; amyloid- $\beta$ ; apoptosis; mitochondrial dysfunction; reactive nitrogen species; reactive oxygen species; regucalcin

## Correspondence

T. Murata, Laboratory of Analytical Neurobiology, Faculty of Pharmacy, Meijo University, Yagotoyama 150, Tempaku, Nagoya 468-8503, Japan  
Fax: +81-52-834-8090  
Tel: +81-52-839-2723  
E-mail: tomiyasu@meijo-u.ac.jp

(Received 8 May 2017, revised 25 November 2017, accepted 12 December 2017)

doi:10.1002/2211-5463.12374

Amyloid- $\beta$  (A $\beta$ ), a primary component of amyloid plaques, has been widely associated with the pathogenesis of Alzheimer's disease. The Ca<sup>2+</sup>-binding protein regucalcin (RGN) plays multiple roles in maintaining cell functions by regulating intracellular calcium homeostasis, various signaling pathways, and gene expression systems. Here, we investigated the functional role of RGN against A $\beta$ -induced cytotoxicity in neuronally differentiated PC12 cells. Overexpression of RGN reduced A $\beta$ -induced apoptosis by reducing mitochondrial dysfunction and caspase activation. It also attenuated A $\beta$ -induced reactive oxygen species production and oxidative damage and decreased A $\beta$ -induced nitric oxide (NO) overproduction, upregulation of inducible NO synthase by nuclear factor- $\kappa$ B, and nitrosative damage. Interestingly, the genetic disruption of RGN increased the susceptibility of neuronally differentiated PC12 cells to A $\beta$  toxicity. Thus, RGN possesses antioxidant activity against A $\beta$ -induced oxidative and nitrosative stress and may play protective roles against A $\beta$ -induced neurotoxicity in Alzheimer's disease.

Regucalcin (RGN) is a Ca<sup>2+</sup>-binding protein that lacks the typical EF-hand Ca<sup>2+</sup>-binding domain [1,2], and was also identified as senescence marker protein-30, which is downregulated with aging in rat livers [3]. Ca<sup>2+</sup>-binding by human RGN was also confirmed in crystal structure and X-ray diffraction analyses [4]. Human and rat RGN genes are localized on the X chromosome and comprise seven exons and six introns [5,6]. Moreover, coding regions of vertebrate RGN are highly conserved [7] and the 5'-flanking region of the RGN gene contains several consensus regulatory elements. Accordingly, the transcription factors AP-1, NF1-A1, RGPR-p117, and  $\beta$ -catenin have been shown to induce RGN gene promoter activity [8]. RGN mRNA and

protein expression was initially detected at high levels in liver and kidney tissues, and was then identified in various other tissues and was shown to be regulated by factors including calcium, calcitonin, parathyroid hormone, 1,25-dihydroxyvitamin D<sub>3</sub>, insulin, tumor necrosis factor- $\alpha$ , transforming growth factor- $\beta$ , estrogen, testosterone, aldosterone, dexamethasone, 17 $\beta$ -estradiol, and 5 $\alpha$ -dihydrotestosterone [9–11].

Regucalcin is known to play multiple regulatory roles in mammalian cells. In particular, intracellular Ca<sup>2+</sup> homeostasis is regulated by RGN via the activities of plasma membrane Ca<sup>2+</sup>-ATPase, sarco-/endoplasmic reticulum Ca<sup>2+</sup>-ATPase, nuclear outer membrane Ca<sup>2+</sup> pump, and mitochondrial Ca<sup>2+</sup> uniporters in many cell

## Abbreviations

O<sub>2</sub><sup>-</sup>, superoxide; A $\beta$ , amyloid- $\beta$ ; iNOS, inducible nitric oxide synthase; NF- $\kappa$ B, nuclear factor- $\kappa$ B; NGF, nerve growth factor; NO, nitric oxide; ONOO<sup>-</sup>, peroxynitrite; ROS, reactive oxygen species; sgRNA, single-guide RNA; TUNEL, terminal deoxynucleotidyl transferase biotin-dUTP nick-end labeling.

types [12]. RGN also regulates the intracellular Ca<sup>2+</sup> signaling enzymes 5'-nucleotidase, adenosine 5'-triphosphatase, cAMP phosphodiesterase, protein kinase C, nitric oxide (NO) synthase, Ca<sup>2+</sup>/calmodulin protein kinase, phosphatase, and calpain, suggesting roles in various intracellular signaling pathways [13–15]. Finally, RGN reportedly controls protein turnover by suppressing protein and nucleic acid synthesis and by activating proteases [13–15].

Several studies have shown that RGN suppresses cell proliferation through multiple signaling pathways [13–15]. Furthermore, RGN may act as a suppressor protein that mitigates human carcinogenesis [16]. Previously, we showed that RGN mRNA is downregulated in human tumor tissues *in vivo* [17], and subsequently, increased RGN gene expression is associated with prolonged survival of patients with pancreatic cancer, breast cancer, and hepatocarcinoma [18–20]. Moreover, the overexpression of human RGN suppressed the proliferation of human pancreatic cancer PaCa-2 cells, human breast cancer MDA-MB-231 cells, and human hepatocellular carcinoma HepG2 cells [18–20].

Alzheimer's disease is a neurodegenerative disease that is characterized by progressive declines in cognitive function, learning, and memory [21,22]. Excessive accumulation of amyloid- $\beta$  (A $\beta$ ) in brain cells is the key defining event in the pathogenesis of Alzheimer's disease, reflecting the neurotoxicity of A $\beta$ , which is a major protein component of senile plaques [23,24]. Ca<sup>2+</sup> signaling in neurons is central to neuronal functions, such as synaptic plasticity, learning, and memory. Hence, disruptions of Ca<sup>2+</sup> transport through Ca<sup>2+</sup> channels on plasma membranes, mitochondria, and the endoplasmic reticulum contribute to neurodegeneration and the development of Alzheimer's disease [25,26]. A $\beta$  has been shown to elevate intracellular Ca<sup>2+</sup> concentrations by inducing Ca<sup>2+</sup> influx, leading to Ca<sup>2+</sup>-mediated neurotoxicity [27,28]. The neurofibrillary pathogenesis of Alzheimer's disease involves tau hyperphosphorylation by Ca<sup>2+</sup>/calmodulin-dependent protein kinase and cytoskeletal protein cleavage by Ca<sup>2+</sup>-dependent protease calpains [29–31]. Because RGN is a reported functional inhibitor of Ca<sup>2+</sup>/calmodulin-dependent protein kinase [32] and calpains [33,34], dysregulation of neuronal Ca<sup>2+</sup> homeostasis during age-related cognitive declines and neurodegenerative disease may be associated with decreased RGN expression [35].

Numerous studies indicate that A $\beta$ -mediated oxidative stress and mitochondrial damage are involved in the pathogenesis of Alzheimer's disease [36–38]. Specifically, A $\beta$  triggers oxidative stress in neuronal cells, in which mitochondrial dysfunction is accompanied by the production of reactive oxygen species (ROS) such as

superoxide (O<sub>2</sub><sup>-</sup>) and hydrogen peroxide (H<sub>2</sub>O<sub>2</sub>). [39–41]. In addition, A $\beta$  reportedly causes nitrosative stress in neuronal cells, in which inducible nitric oxide synthase (iNOS) produces reactive nitrogen species such as NO and peroxynitrite (ONOO<sup>-</sup>) [42–44]. The consequent oxidative and/or nitrosative stress contributes to neuronal damage and leads to the formation of advanced glycation end products, advanced lipid peroxidation end products, and oxidized nucleic acids in Alzheimer's disease [38,40,45]. Herein, we investigated the protective effects of RGN against A $\beta$ -induced neurotoxicity in neuronally differentiated PC12 cells and characterized the underlying neuroprotective mechanisms of action.

## Materials and methods

### Materials

The following materials from the indicated sources were used in this study: Dulbecco's modified Eagle's medium (DMEM), Dulbecco's PBS (DPBS), fetal bovine serum (FBS), horse serum (HS), penicillin, streptomycin, MitoSOX Red, tetramethylrhodamine methyl ester (TMRM) and 5-(and-6)-chloromethyl-2',7'-dichlorodihydrofluorescein diacetate acetyl ester (CM-H<sub>2</sub>DCFDA) from Invitrogen (Carlsbad, CA, USA); rat nerve growth factor (NGF) and caspase fluorescence assay kit from R&D Systems, Inc. (Minneapolis, MN, USA); A $\beta$ <sub>25–35</sub> and Hoechst 33342 dye from Sigma-Aldrich (St. Louis, MO, USA); pMXs-puro retrovirus vector, Platinum-E retrovirus packaging cells, and OxiSelect Nitrotyrosine ELISA kit from Cell Biolabs (San Diego, CA, USA); NeuroMag and ViroMag R/L viral gene delivery reagent from OZ Biosciences (Marseille, France); lipid peroxidation assay kit from BioVision (Milpitas, CA, USA); NO assay kit from Dojin (Kumamoto, Japan); Pierce BCA protein assay reagent kit from Thermo Scientific (Waltham, MA, USA); pGL4.32[luc2P/nuclear factor- $\kappa$ B (NF- $\kappa$ B)-RE/Hygro] vector, pRL-TK vector, and Dual-Glo luciferase assay system from Promega (Madison, WI, USA); rabbit anti-iNOS antibody from Cell Signaling Technology (Danvers, MA, USA); peroxidase-conjugated donkey anti-rabbit IgG antibody and enhanced chemiluminescent (ECL) western blotting detection reagents from Amersham Biosciences (Piscataway, NJ, USA); protease and phosphatase inhibitor cocktail tablets and *in situ* apoptosis detection kit from Roche (Mannheim, Germany); and lentiviral vectors containing a single-guide RNA (sgRNA)/CRISPR/Cas9 All-in-One gene targeting system from Applied Biological Materials (Richmond, Canada).

### Cell culture and retrovirus infection

Pheochromocytoma PC12 cells were obtained from RIKEN BRC Cell Bank (Ibaraki, Japan) and then subcloned to

generate more homogeneous populations. PC12 cells were cultured in DMEM supplemented with 5% heat-inactivated FBS, 5% HS, 50 units·mL<sup>-1</sup> penicillin, and 50  $\mu$ g·mL<sup>-1</sup> streptomycin in a humidified atmosphere of 5% CO<sub>2</sub> and 95% air. Mouse RGN and  $\beta$ -galactosidase (LacZ) cDNA were subcloned into the pMXs-puro retrovirus vector. Vectors were transfected into Plat-E retrovirus packaging cells, and PC12 cells were infected with retrovirus in the presence of ViroMag R/L viral gene delivery reagent. In RGN knockout manipulations using CRISPR/Cas9/sgRNA technology, sgRNA sequences targeting RGN were 5'-GATTGCTGATCGAATCCCAT-3', 5'-CGAGTGCAGC-GAGTTGGTGT-3', and 5'-AGGTACCATGGCTGAG-GAAA-3', and a scramble sgRNA was used as a control sgRNA. A mixture of three types of lentiviruses expressing sgRNA against RGN was used to transduce PC12 cells. Retrovirus- or lentivirus-infected cells were selected with puromycin (3  $\mu$ M) for 3 weeks and were then used in experiments. PC12 cells were neuronally differentiated by treatment with NGF (100 ng·mL<sup>-1</sup>) in DMEM containing 1% HS. After selection by incubation with puromycin, neuronal differentiation of PC12 cells was induced by NGF (100 ng·mL<sup>-1</sup>) in DMEM containing 1% HS. Subsequently, A $\beta$ <sub>25-35</sub> peptide was dissolved in deionized water at 1 mM, applied to cells at 37 °C overnight to promote fibril formation, and then stored at -80 °C.

### Assay of apoptotic cells

DNA fragmentation was estimated using terminal deoxynucleotidyl transferase biotin-dUTP nick-end labeling (TUNEL) assays with an *in situ* apoptosis detection kit according to the manufacturer's instructions. Briefly, after treatment in chamber slides, cells were washed three times with ice-cold DPBS and were fixed with 4% paraformaldehyde for 10 min. Cells were then washed twice in DPBS and were permeabilized using 0.1% Triton X-100 in 0.1% sodium citrate for 10 min. Subsequently, cells were incubated with the TUNEL reaction mixture for 1 h at 37 °C in the dark. After washing twice with DPBS, nuclear counterstaining was performed with Hoechst 33342 dye (10  $\mu$ g·mL<sup>-1</sup>) to determine total cell counts. Numbers of TUNEL-positive cells per 500 cells were counted in randomly selected fields using a Zeiss fluorescence microscope (Carl Zeiss MicroImaging, Inc., Jena, Germany).

### Measurement of mitochondrial membrane potential

Mitochondrial membrane potential was measured using the fluorescent dye TMRM. Briefly, cells were treated in chamber slides and incubated in a medium containing TMRM (200 nM) for 20 min, washed with DPBS containing Hoechst 33342 dye (10  $\mu$ g·mL<sup>-1</sup>) and then with DPBS alone, and then placed in phenol red-free DMEM. Cells

were then visualized using a Zeiss fluorescence microscope, and pictures were taken of random fields of view. Fluorescent intensities of TMRM were quantified using Zeiss software (Carl Zeiss MicroImaging, Inc., Jena, Germany).

### Assay of caspase activity

Caspase activities were measured using fluorescent substrates as described previously [46] with minor modifications. Briefly, caspase-9 and caspase-3 activities were measured using a caspase fluorescence assay kit according to the manufacturer's instructions. Briefly, after treatment on 24-well dishes, cells were washed with ice-cold DPBS and were lysed in caspase lysis buffer for 15 min on ice. Cells were then centrifuged at 15 000 *g* for 15 min at 4 °C, and protein concentrations of supernatants were determined using micro-BCA protein assay reagent kits. Supernatants containing 50  $\mu$ g of protein were then incubated with 50  $\mu$ M LEHD-AFC (caspase-9 substrate) or DEVD-AFC (caspase-3 substrate) for 1 h, and caspase activities were assayed using fluorometric determinations of the hydrolyzed products with a Perkin Elmer microplate spectrofluorometer (EnSpire, Norwalk, CT, USA) at excitation and emission wavelengths of 400 and 505 nm, respectively. Enzyme activities were expressed as fluorescence intensities in arbitrary units (a.u.) per mg of total protein.

### Measurement of mitochondrial and intracellular ROS

Mitochondrial ROS generation was visualized using the fluorescent dye MitoSOX Red, which is sensitive to O<sub>2</sub><sup>-</sup>. Intracellular ROS generation was also visualized using the fluorescent dye CM-H<sub>2</sub>DCFDA, which is particularly sensitive to H<sub>2</sub>O<sub>2</sub> among various ROS. In these experiments, cells were treated in chamber slides, then incubated in medium containing MitoSOX Red (5  $\mu$ M) or CM-H<sub>2</sub>DCFDA (5  $\mu$ M) for 30 min, washed with DPBS containing Hoechst 33342 dye (10  $\mu$ g·mL<sup>-1</sup>) and then with DPBS alone, and then placed in phenol red-free DMEM. Cells were visualized using a Zeiss fluorescence microscope, and pictures were taken of randomly selected fields of view. Fluorescent intensities of MitoSOX and CM-H<sub>2</sub>DCFDA were quantified using Zeiss software.

### Assay of lipid peroxidation

Oxidative damage was assayed by measuring malondialdehyde concentrations using a lipid peroxidation assay kit according to the manufacturer's protocol. Briefly, after treatment, cells were washed with DPBS, harvested by trypsinization, and then sonicated for 20 s in malondialdehyde lysis buffer. After centrifugation at 13 000 *g* for 10 min, supernatants were incubated with thiobarbituric acid at 95 °C for 1 h and were then cooled to room

temperature. Subsequently, samples were transferred to 96-well plates for fluorometric analyses with a Perkin Elmer microplate spectrofluorometer. Protein concentrations of supernatants were determined using a micro-BCA protein assay reagent kit. Malondialdehyde contents were normalized to mg of total protein.

### Measurement of NO production

Nitric oxide production was estimated from nitrite contents that were detected using NO assay kits with the Griess reaction according to the manufacturer's instructions. After treatment on 24-well dishes, culture media were mixed with Griess reagent and incubated for 20 min at room temperature. Subsequently, absorbances of mixtures were determined at 540 nm using a Perkin Elmer microplate spectrofluorometer.

### Immunoblot analysis of iNOS expression

After treatment on 35-mm dishes, cells were lysed in RIPA lysis buffer containing the protease inhibitor mixture. Lysed cells were then centrifuged at 15 000 *g* for 15 min at 4 °C, and protein concentrations of supernatants were determined using micro-BCA protein assay reagent kits. Supernatants containing 50  $\mu$ g of protein were then boiled in Laemmli sample buffer containing 5% 2-mercaptoethanol. Proteins were resolved using 12% sodium dodecyl sulfate/polyacrylamide gel electrophoresis and were transferred to polyvinylidene difluoride membranes. After blocking for 1 h in buffer containing 20 mM Tris/HCl (pH 7.6), 100 mM NaCl, 0.1% Tween-20 (TBS-T), and 3% skim milk, membranes were incubated with rabbit anti-iNOS antibody (1 : 100) in TBS-T containing 1% skim milk and then with peroxidase-conjugated donkey anti-rabbit IgG antibody in the same buffer. Bound antibody was visualized using the ECL system. Blots were then stripped and reprobed with anti- $\beta$ -actin antibody to use  $\beta$ -actin as a loading control.

### Assay of transcriptional activity of nuclear factor- $\kappa$ B (NF- $\kappa$ B)

Nuclear factor- $\kappa$ B transcriptional activity was determined by a reporter gene assay as described previously [46] with minor modifications. Briefly, the transcriptional activity of NF- $\kappa$ B was measured after transfecting cells with the pRL-TK vector (0.125  $\mu$ g per well) and the NF- $\kappa$ B-TA-Luc vector (0.5  $\mu$ g per well) or the molar equivalent of the pTA-Luc vector (negative control). Transfection was performed with the NeuroMag reagent according to the manufacturer's instructions. The pRL-TK vector contains the *Renilla* luciferase gene under the control of the minimum promoter from herpes simplex virus thymidine kinase, and was used as an internal control for differences in transfection efficiencies and cell numbers. After transfection, cells

were treated in DMEM with or without A $\beta$  for various times. Transfected cells were then lysed, and luciferase activities of lysates were measured using dual-luciferase assays according to the manufacturer's instructions. Reporter gene activity was expressed as firefly luciferase activity of the NF- $\kappa$ B-TA-Luc vector divided by *Renilla* luciferase activity of the pRL-TK vector. Luciferase activity of the pTA-Luc vector was subtracted from that of the NF- $\kappa$ B-TA-Luc vector.

### Measurements of nitrotyrosine contents

Intracellular ONOO<sup>-</sup> formation was investigated as an indicator of nitrosative stress by determining intracellular 3-nitrotyrosine contents using OxiSelect Nitrotyrosine ELISA kits according to the manufacturer's instructions. Briefly, cells were treated on 24-well dishes and were then washed with ice-cold DPBS and lysed in RIPA buffer containing protease and phosphatase inhibitor mixtures for 15 min on ice. After centrifugation at 15 000 *g* for 15 min at 4 °C, supernatants were collected and nitrotyrosine contents were normalized to mg of total protein, which were determined using micro-BCA protein assay reagent kits.

### Statistical analysis

The significance of differences was estimated with Student's *t*-test using GraphPad Prism software (GraphPad software, Inc., San Diego, CA, USA). A *P* value of < 0.05 was considered significant.

## Results and Discussion

After retrovirus-mediated gene transfer of RGN or LacZ, infected cells were selected using puromycin treatments. Subsequently, we determined whether RGN modulates A $\beta$ -induced apoptosis in neuronally differentiated PC12 cells by measuring apoptotic responses to A $\beta$  using TUNEL staining analyses (Fig. 1A). In these experiments, numbers of apoptotic cells in LacZ-overexpressing control cells were significantly increased after A $\beta$  treatment in a time-dependent manner. Compared with LacZ control cells, numbers of A $\beta$ -induced apoptotic cells were fewer among RGN-overexpressing cells, suggesting that RGN protects against A $\beta$ -induced apoptosis in neuronally differentiated PC12 cells.

Previous studies show that A $\beta$  reduces mitochondrial membrane potential in neuronal cells, indicating mitochondrial dysfunction under these conditions [36–38]. Accordingly, we examined the effects of RGN overexpression on A $\beta$ -induced loss of mitochondrial membrane potential in neuronally differentiated PC12

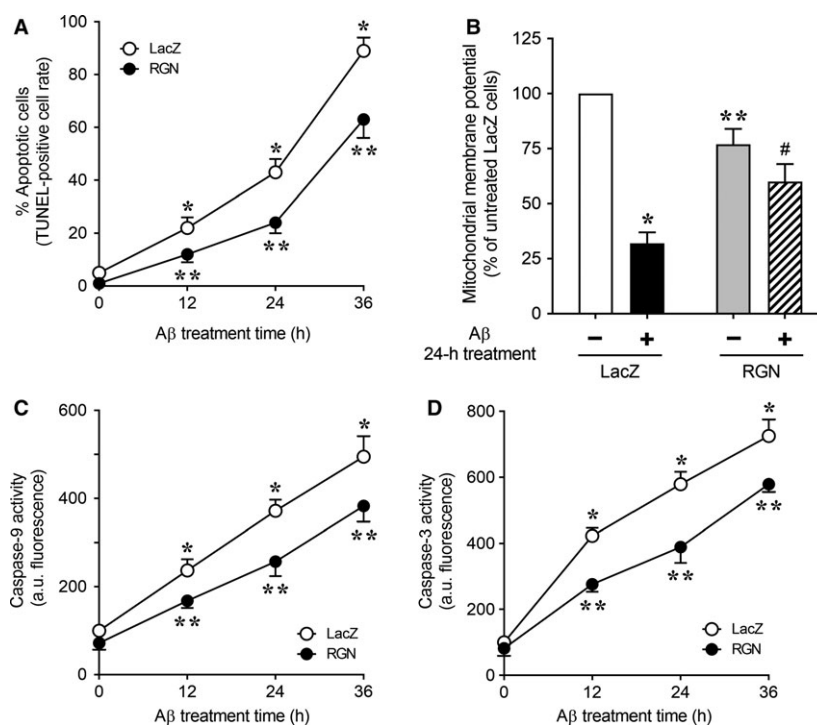


**Fig. 1.** Regucalcin attenuates A $\beta$ -induced apoptosis by activating the mitochondrial caspase pathway in neuronally differentiated PC12 cells. NGF-differentiated PC12 cells overexpressing  $\beta$ -galactosidase (LacZ) or RGN were treated with 25  $\mu$ M A $\beta$  for the indicated periods. (A) Cells were incubated with the TUNEL reaction mixture to determine rates of apoptosis and then stained with the Hoechst 33342 nuclear stain. TUNEL-positive apoptotic nuclei were identified using a fluorescent microscope. (B) Mitochondrial membrane potential was measured using the fluorescent probe TMRE. (C,D) Caspase-9-mediated cleavage of LEHD-AFC and caspase-3-mediated cleavage of DEVD-AFC were estimated in cell lysates using fluorometric assays with specific substrates. Data are expressed as mean a.u. of fluorescence/mg protein  $\pm$  standard errors of the mean (SE) from three independent RGN experiments performed in triplicate. (A) \* $P$  < 0.05, A $\beta$ -treated RGN cells versus untreated LacZ cells at time 0; \*\* $P$  < 0.05, A $\beta$ -treated LacZ cells versus untreated LacZ cells; \*\*\* $P$  < 0.05, untreated RGN cells versus untreated LacZ cells; # $P$  < 0.05, A $\beta$ -treated RGN cells versus A $\beta$ -treated LacZ cells; (C and D) \* $P$  < 0.05, A $\beta$ -treated LacZ cells versus untreated LacZ cells at time 0; \*\* $P$  < 0.05, A $\beta$ -treated RGN cells versus A $\beta$ -treated LacZ cells at the same time point.

cells (Fig. 1B). We confirmed A $\beta$ -induced decreases in mitochondrial membrane potential in LacZ-overexpressing control cells and observed slightly lower mitochondrial membrane potential in untreated RGN-overexpressing cells than in untreated LacZ-overexpressing cells. However, following treatment with A $\beta$ , RGN-overexpressing cells had significantly higher mitochondrial membrane potential than LacZ-overexpressing cells, and no significant differences in mitochondrial DNA copy numbers were observed (data not shown). These results indicate that RGN blocks the induction of mitochondrial dysfunction by A $\beta$ , as characterized by loss of mitochondrial membrane potential. It is widely accepted that A $\beta$ -mediated loss of mitochondrial membrane potential promotes mitochondrial apoptosis, during which cytoplasmic release of cytochrome *c* activates caspase-9 and downstream caspase-3 [47]. Thus, we examined time-dependent changes in caspase activity in neuronally differentiated

PC12 cells overexpressing LacZ or RGN following treatment with A $\beta$  (Fig. 1C,D). In these experiments, LacZ-overexpressing cells showed increased caspase-9 and caspase-3 activities following treatment with A $\beta$ , and overexpression of RGN resulted in significant decreases in A $\beta$ -induced activities of both caspases when compared with LacZ-overexpressing control cells. Taken together, these data indicate that RGN attenuates A $\beta$ -induced mitochondrial apoptosis by maintaining mitochondrial membrane potential.

Amyloid- $\beta$ -mediated disruptions of mitochondrial function are prominent early events in Alzheimer's disease. Moreover, A $\beta$  exposure of neuronal cells has been shown to increase intracellular ROS production, which has been strongly associated with mitochondrial dysfunction [39–41]. Mitochondria are the main source of intracellular ROS, likely reflecting production of O $_2^-$  [48] and subsequent conversion into H $_2$ O $_2$  spontaneously or by superoxide dismutase [48]. Hence, we

examined mitochondrial ROS production in LacZ- or RGN-overexpressing cells using the fluorescent dye MitoSOX Red, which is rapidly oxidized by O $_2^-$  (Fig. 2A). In these studies, control cells overexpressing LacZ showed significant increases in mitochondrial ROS after treatment with A $\beta$ . Moreover, untreated RGN-overexpressing cells had significantly lower basal levels of mitochondrial ROS than those overexpressing LacZ. Following treatment with A $\beta$ , RGN-overexpressing cells exhibited significant decreases in mitochondrial ROS production compared with LacZ-overexpressing control cells, suggesting that RGN attenuates basal and A $\beta$ -induced mitochondrial ROS production. In further assays using the intracellular ROS indicator CM-H $_2$ DCFDA, we measured differences in intracellular ROS levels in LacZ- or RGN-overexpressing cells exposed to A $\beta$  (Fig. 2B) and confirmed that RGN overexpression decreases basal and A $\beta$ -induced intracellular ROS production. These results suggest that RGN attenuates basal and A $\beta$ -induced intracellular ROS contents by regulating mitochondrial ROS production.

Regucalcin has been shown to be localized to mitochondria [49], and previous electron microscopy analyses showed abnormally enlarged mitochondria with indistinct cristae in hepatocytes from RGN knockout mice, compared with those in wild-type mice [50]. These reports imply that RGN plays an important role in the maintenance of mitochondrial function. Normal mitochondria mediate redox signaling by releasing ROS from the electron transport chain, and overexpression of RGN decreased mitochondrial ROS production under basal conditions [see Fig. 2A; LacZ (-) versus RGN (-)]. Hence, RGN may preserve electron transport chain activity, leading to a lower mitochondrial membrane potential under basal conditions [Fig. 1B; LacZ (-) versus RGN (-)]. These data suggest that RGN protects neuronal cells from A $\beta$ -mediated neurotoxicity by ameliorating mitochondrial ROS generation.

Amyloid- $\beta$ -induced excessive ROS generation reportedly causes oxidative damage to cell components including lipids, proteins, and DNA and thereby disrupts neuronal cell function [38,40,45]. Thus, to

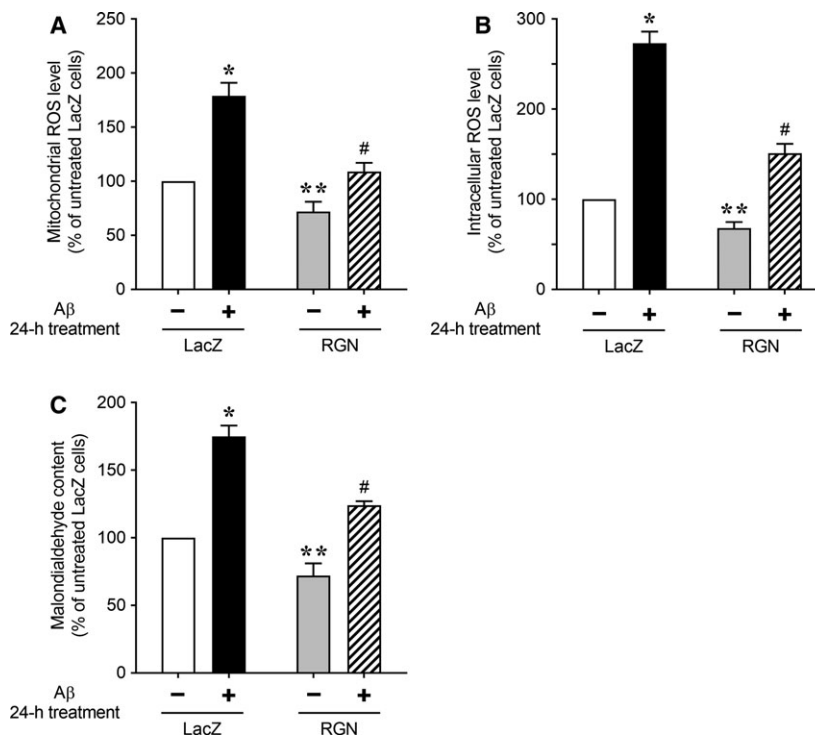


**Fig. 2.** RGN attenuates A $\beta$ -induced oxidative damage in neuronally differentiated PC12 cells. NGF-differentiated PC12 cells overexpressing LacZ or RGN were treated with 25  $\mu$ M A $\beta$  for 24 h. (A) Mitochondrial ROS generation was detected using the fluorescent (O $_2^-$ ) probe MitoSOX Red. (B) Intracellular ROS generation was detected using fluorescent hydrogen peroxide indicator CM-H $_2$ DCFDA. (C) Oxidative damage was estimated by measuring malondialdehyde contents as an index of lipid peroxidation. Data are presented as means  $\pm$  SE of three independent experiments performed in triplicate. \* $P$  < 0.05, A $\beta$ -treated LacZ cells versus untreated LacZ cells; \*\* $P$  < 0.05, untreated RGN cells versus untreated LacZ cells; # $P$  < 0.05, A $\beta$ -treated RGN cells versus A $\beta$ -treated LacZ cells.

determine whether RGN attenuates A $\beta$ -induced oxidative damage, we determined ROS-mediated lipid peroxidation according to concentrations of the end product malondialdehyde (Fig. 2C). Significantly increased levels of lipid peroxidation were observed in A $\beta$ -treated cells overexpressing LacZ relative to untreated LacZ-overexpressing control cells. However, upon treatment with A $\beta$ , RGN-overexpressing cells had significantly lower malondialdehyde levels than LacZ-overexpressing cells, indicating that RGN protects against A $\beta$ -mediated lipid peroxidation.

Published *in vitro* studies show that RGN is cytoprotective against apoptotic cell death induced by tumor necrosis factor- $\alpha$ , lipopolysaccharide, transforming growth factor- $\beta$ 1, and thapsigargin [10,11]. In agreement, previous *ex vivo* studies of seminiferous tubules from transgenic rats showed protective effects of RGN overexpression against tert-butyl hydroperoxide- and cadmium-induced oxidative stress in rat testis [51]. Moreover, *in vivo* studies with RGN knockout mice showed high susceptibility to age- and smoking-related oxidative stress in lungs [52]. These RGN knockout mice also had elevated oxidative stress in the brain [53]. Thus, RGN likely plays important roles in cell defenses against oxidative stress. Furthermore, RGN expression is decreased with aging in the cerebral cortex and hippocampus [54], further indicating that age-related decreases in RGN expression contribute to A $\beta$ -mediated oxidative stress and neurotoxicity in Alzheimer's disease.

In addition to oxidative damage, nitrosative damage due to overproduction of NO has been associated with the pathophysiology of Alzheimer's disease [55,56]. In particular, the exposure of neuronal cells to A $\beta$  led to NO overproduction by upregulating iNOS [57–60]; in other studies, A $\beta$  caused NO-mediated nitrosative damage in neuronal cells [42–44]. Accordingly, we examined the effects of RGN overexpression on NO production in neuronally differentiated PC12 cells in the presence of A $\beta$  (Fig. 3A) and showed significantly greater NO production following treatment of LacZ-overexpressing control cells with A $\beta$ . In separate experiments, RGN-overexpressing cells exhibited significant decreases in NO production following exposure to A $\beta$  when compared with LacZ-overexpressing control cells.

Amyloid- $\beta$ -induced NO production was previously shown to follow upregulation of iNOS mRNA by the transcription factor NF- $\kappa$ B [60]. Hence, to further investigate the roles of RGN in iNOS expression and NF- $\kappa$ B activity, we examined whether iNOS protein levels and NF- $\kappa$ B activity are altered by overexpression of RGN (Fig. 3B,C). In these experiments,

exposure of LacZ-expressing control cells to A $\beta$  resulted in increases in both iNOS expression and NF- $\kappa$ B activity. In contrast, RGN overexpression led to significantly lower A $\beta$ -induced iNOS expression and NF- $\kappa$ B activity than in LacZ-overexpressing control cells, indicating that RGN inhibits A $\beta$ -induced NO overproduction by attenuating NF- $\kappa$ B-mediated iNOS expression.

Intracellular NO reacts rapidly with O $_2^-$  to produce the powerful oxidant ONOO $^-$ , which is a major causal factor in NO-mediated neurotoxicity [42–44]. Because ONOO $^-$  selectively nitrates tyrosine residues of proteins [45,56], we estimated the effects of RGN overexpression on A $\beta$ -induced intracellular nitrotyrosine levels. These experiments showed increased intracellular nitrotyrosine levels in A $\beta$ -treated LacZ-overexpressing control cells and significantly attenuated A $\beta$ -induced nitrotyrosine production in RGN-overexpressing cells. Taken together, these results suggest that RGN reduces A $\beta$ -induced nitrosative cell damage by reducing the production of reactive nitrogen species such as NO and ONOO $^-$ .

To further investigate the protective effect of RGN on A $\beta$  toxicity in PC12 neuron-like cells, we used the CRISPR/Cas9 technique to disrupt the RGN gene in PC12 cells and then examined the sensitivity of RGN knockout PC12 cells to A $\beta$ . RGN expression was induced by the treatment of PC12 cells with NGF (data not shown). As shown in Fig. 4A, the immunoblot analysis of neuronally differentiated PC12 cells expressing scramble sgRNA confirmed the presence of endogenous RGN protein. In contrast, endogenous RGN protein was not detected in neuronally differentiated PC12 cells expressing sgRNA targeting RGN, indicating successful RGN gene knockout in PC12 cells. As shown in Fig. 4B, the cells expressing sgRNA targeting RGN potentiated A $\beta$ -induced increases in numbers of apoptotic cells when compared with control cells expressing scramble sgRNA. In addition, because we found that A $\beta$  activates the caspase-9/3 cascade via mitochondrial dysfunction, as indicated by decreases in mitochondrial membrane potential (see Fig. 1B–D), we examined the effects of RGN loss on the A $\beta$ -induced activation of the caspase-9/3 cascade (Fig. 4C,D). The cells expressing sgRNA targeting RGN exhibited significant increases in the A $\beta$ -induced activity of caspase-9 and caspase-3 when compared with control cells expressing scramble sgRNA, suggesting that RGN deficiency exacerbates A $\beta$ -induced apoptosis by activating the caspase-9/3 cascade via mitochondrial dysfunction. Moreover, because we found that A $\beta$  increased mitochondrial ROS production, which leads to an increase in intracellular ROS level and subsequent oxidative

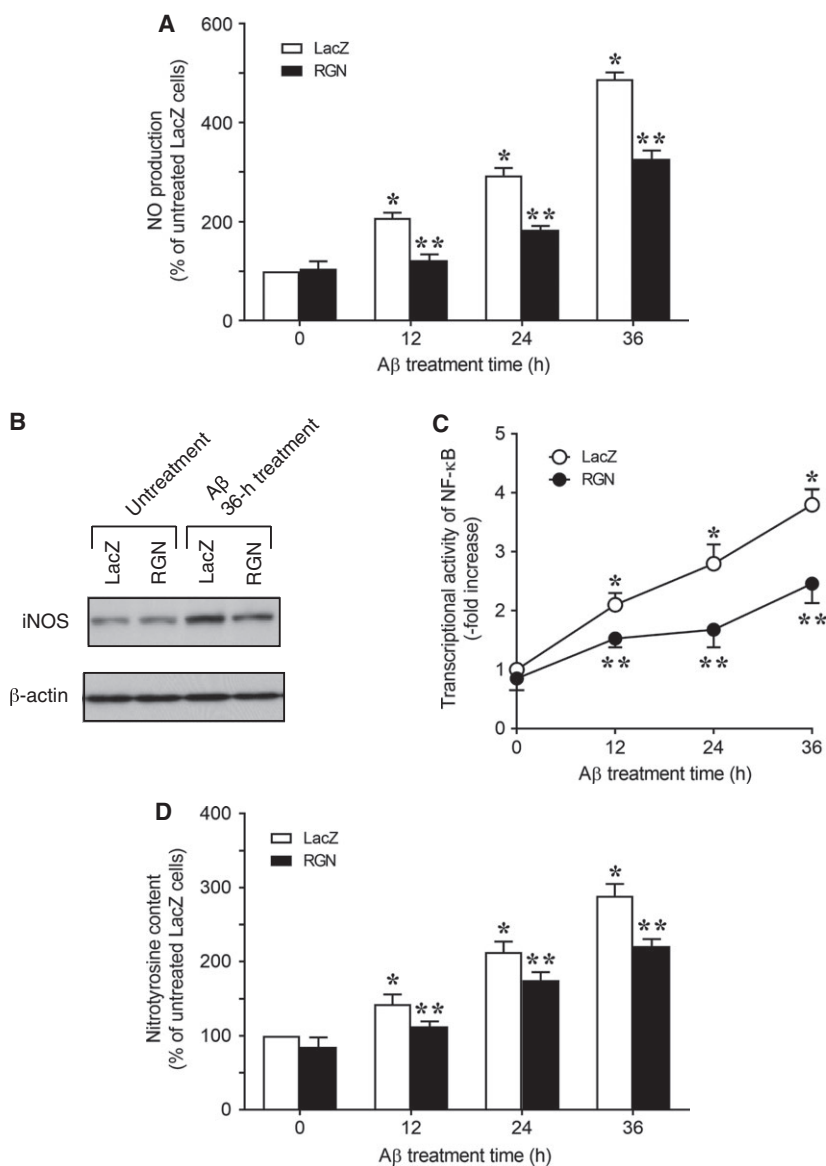


**Fig. 3.** RGN attenuates A $\beta$ -induced nitrosative damage in neuronally differentiated PC12 cells. NGF-differentiated PC12 cells overexpressing LacZ or RGN were treated with 25  $\mu$ M A $\beta$  for the indicated time periods. (A) NO contents of medium were measured using the Griess method. (B) iNOS protein expression was determined using western blotting with a specific antibody. Actin expression was used as a protein loading control. (C) Cells were transiently cotransfected with a NF- $\kappa$ B-responsive reporter vector and the internal control vector pRL-TK. After 12 h, transfected cells were treated with A $\beta$  for the indicated periods and were then lysed for NF- $\kappa$ B reporter assays with a dual-luciferase reporter assay system. Data are presented as fold increases compared with luciferase activity at 0 h in LacZ cells, which was set at 1.0. (D) Nitrosative damage was estimated by measuring content of nitrotyrosine, which indicates the nitration of tyrosine by ONOO<sup>-</sup> generated from NO and O<sub>2</sub><sup>-</sup>. Data are presented as means  $\pm$  SE of three independent experiments performed in triplicate. (A, C, and D) \* $P$  < 0.05, A $\beta$ -treated LacZ cells versus untreated LacZ cells at time 0; \*\* $P$  < 0.05, A $\beta$ -treated RGN cells versus A $\beta$ -treated LacZ cells at the same time point.

damage (see Fig. 2A–C), we examined the effect of RGN loss on A $\beta$ -induced increases in mitochondrial ROS production (Fig. 4E). Under untreated conditions, the cells expressing sgRNA targeting RGN showed significant increases in mitochondrial ROS production compared with scramble sgRNA-expressing control cells (see Fig. 4E; A $\beta$  (-)/scramble sgRNA versus A $\beta$  (-)/RGN sgRNA), suggesting that RGN controls mitochondrial ROS generation under basal conditions. Upon treatment with A $\beta$ , mitochondrial ROS production in RGN sgRNA-expressing cells was significantly increased relative to that in scramble sgRNA-expressing control cells (see Fig. 4E; A $\beta$  (+)/scramble sgRNA versus A $\beta$  (+)/RGN sgRNA), suggesting that RGN deficiency enhances A $\beta$ -induced

oxidative stress by increasing mitochondrial ROS production.

Furthermore, because we found that A $\beta$  caused nitrosative cell damage by promoting NO production via NF- $\kappa$ B activation-mediated iNOS expression (see Fig. 3A–D), we examined the effect of RGN loss on A $\beta$ -induced NO production and iNOS expression (Fig. 4F,G). The exposure of cells expressing sgRNA targeting RGN to A $\beta$  caused significant increases in NO production and iNOS expression compared with that in control cells expressing scramble sgRNA. These results suggest that RGN deficiency potentiates A $\beta$ -mediated nitrosative stress by increasing iNOS-mediated NO production. Taken together, the knock-out data described above suggest that RGN protects

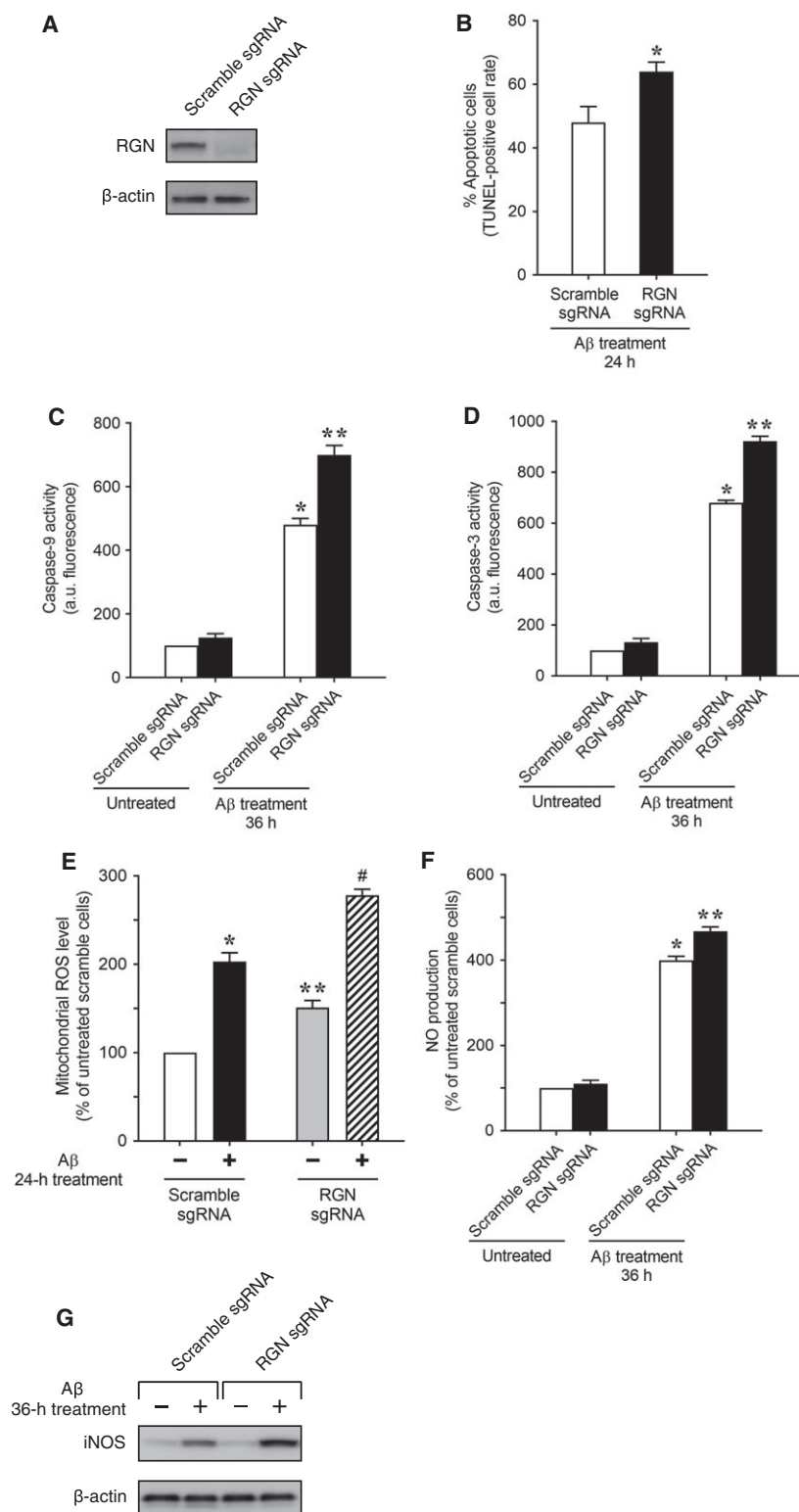


**Fig. 4.** RGN-deficient PC12 neuron-like cells become vulnerable to A $\beta$  toxicity. A lentivirus-mediated CRISPR/Cas9 system was used to generate PC12 cells, in which the RGN gene is knocked out. PC12 cells were infected with lentiviruses harboring RGN sgRNA or control scramble sgRNA, selected with puromycin, and then neuronally differentiated using treatments with NGF. (A) Knockdown efficiency was examined by western blotting using  $\beta$ -actin as a loading control. (B–F) Upon treatment with A $\beta$ , apoptosis assay, caspase assay, mitochondrial ROS measurement, NO assay, and iNOS western blotting were performed as described in the legends to Figs 1A,C,D, 2A and 3A,B, respectively. Data are presented as means  $\pm$  SE of three independent experiments performed in triplicate. (B)  $*P < 0.05$ , A $\beta$ -treated RGN sgRNA cells versus A $\beta$ -treated scramble sgRNA cells; (C,D)  $*P < 0.05$ , A $\beta$ -treated scramble sgRNA cells versus untreated scramble sgRNA cells;  $**P < 0.05$ , A $\beta$ -treated RGN sgRNA cells versus A $\beta$ -treated scramble sgRNA cells; (E)  $*P < 0.05$ , A $\beta$ -treated scramble sgRNA cells versus untreated scramble sgRNA cells;  $**P < 0.05$ , untreated RGN sgRNA cells versus untreated scramble sgRNA cells;  $*P < 0.05$ , A $\beta$ -treated RGN sgRNA cells versus A $\beta$ -treated scramble sgRNA cells; (F)  $*P < 0.05$ , A $\beta$ -treated scramble sgRNA cells versus untreated scramble sgRNA cells;  $**P < 0.05$ , A $\beta$ -treated RGN sgRNA cells versus A $\beta$ -treated scramble sgRNA cells.

PC12 neuron-like cells from A $\beta$ -induced apoptosis based on oxidative and nitrosative stresses. Thus, consistent with our findings from RGN overexpression

experiments, the effects of RGN knockout provide further evidence of the protective function of RGN against A $\beta$  toxicity.

In the present study, we demonstrate that RGN attenuates the susceptibility of neuronally differentiated PC12 cells to A $\beta$ -induced apoptosis. We also showed that RGN prevents oxidative and nitrosative A $\beta$  toxicity in neuronally differentiated PC12 cells. Thus, RGN may play an important protective role in neurons of patients with Alzheimer's disease, and our findings provide novel insights into cellular defense mechanisms against A $\beta$  neurotoxicity. Further *in vivo* studies are required to determine whether RGN protects neuronal cells from the A $\beta$  toxicity that occurs in Alzheimer's disease. Thus, because we previously generated transgenic rats overexpressing RGN [61], it will be valuable to determine whether RGN transgenic rats are more or less sensitive than control rats to intracerebroventricular injections of A $\beta$ . In addition, the present data from RGN overexpression experiments warrant determinations of whether virus-mediated RGN gene transfer reverses pathologic changes and behavioral deficits in mouse models of A $\beta$ -mediated Alzheimer's disease. Furthermore, the present RGN knockout data indicate the value of experiments designed to determine whether brain-specific RGN-deficient mice exhibit neuronal vulnerability to A $\beta$  toxicity. Finally, a previous report showed that the natural product compound EUK4010 inhibits A $\beta$ -induced neuronal cell damage and attenuates A $\beta$ -mediated suppression of RGN [62]. Taken together, these data warrant consideration of RGN as a therapeutic target for A $\beta$ -mediated neuronal toxicity. Specifically, further investigations of the protective effects of RGN against A $\beta$  neurotoxicity may lead to the development of novel neuroprotective strategies for the treatment of Alzheimer's disease.

## Acknowledgements

This work was partly supported by a Grant-in-Aid for Scientific Research (C) (16K08252) from the Ministry of Education, Culture, Sports, Science and Technology (MEXT) of Japan and by Matching Fund Subsidy for Private Universities from MEXT for purchasing the confocal laser scanning fluorescence microscopy.

## Author contributions

TM, MK, YS, MK, and KH performed the experiments, SK and CT constructed retrovirus expression system, and TM and MY designed the experiment and discussed with NK. MY provided comments pertaining to the manuscript. TM wrote the manuscript. All authors read and commented on the manuscript.

## References

- 1 Yamaguchi M and Yamamoto T (1978) Purification of calcium binding substance from soluble fraction of normal rat liver. *Chem Pharm Bull* **26**, 1915–1918.
- 2 Shimokawa N and Yamaguchi M (1993) Molecular cloning and sequencing of the cDNA coding for a calcium-binding protein regucalcin from rat liver. *FEBS Lett* **327**, 251–255.
- 3 Fujita T, Uchida K and Maruyama N (1992) Purification of senescence marker protein-30 (SMP30) and its androgen-independent decrease with age in the rat liver. *Biochim Biophys Acta* **1116**, 122–128.
- 4 Chakraborti S and Bahnsen BJ (2010) Crystal structure of human senescence marker protein 30: insights linking structural, enzymatic, and physiological functions. *Biochemistry* **49**, 3436–3444.
- 5 Fujita T, Mandel JL, Shirasawa T, Hino O, Shirai T and Maruyama N (1995) Isolation of cDNA clone encoding human homologue of senescence marker protein-30 (SMP30) and its location on the X chromosome. *Biochim Biophys Acta* **1263**, 249–252.
- 6 Shimokawa N, Matsuda Y and Yamaguchi M (1995) Genomic cloning and chromosomal assignment of rat regucalcin gene. *Mol Cell Biochem* **151**, 157–163.
- 7 Misawa H and Yamaguchi M (2000) The gene of Ca<sup>2+</sup>-binding protein regucalcin is highly conserved in vertebrate species. *Int J Mol Med* **6**, 191–196.
- 8 Yamaguchi M (2011) The transcriptional regulation of regucalcin gene expression. *Mol Cell Biochem* **346**, 147–171.
- 9 Yamaguchi M (2011) Regucalcin and cell regulation: role as a suppressor protein in signal transduction. *Mol Cell Biochem* **353**, 101–137.
- 10 Yamaguchi M (2013) The anti-apoptotic effect of regucalcin is mediated through multisignaling pathways. *Apoptosis* **18**, 1145–1153.
- 11 Marques R, Maia CJ, Vaz C, Correia S and Socorro S (2014) The diverse roles of calcium-binding protein regucalcin in cell biology: from tissue expression and signalling to disease. *Cell Mol Life Sci* **71**, 93–111.
- 12 Yamaguchi M (2000) Role of regucalcin in calcium signaling. *Life Sci* **66**, 1769–1780.
- 13 Yamaguchi M (2000) The role of regucalcin in nuclear regulation of regenerating liver. *Biochem Biophys Res Commun* **276**, 1–6.
- 14 Yamaguchi M (2005) Role of regucalcin in maintaining cell homeostasis and function. *Int J Mol Med* **15**, 371–389.
- 15 Yamaguchi M (2013) Role of regucalcin in cell nuclear regulation: involvement as a transcription factor. *Cell Tissue Res* **354**, 331–341.
- 16 Yamaguchi M (2015) Involvement of regucalcin as a suppressor protein in human carcinogenesis: insight into

- the gene therapy. *J Cancer Res Clin Oncol* **141**, 1333–1341.
- 17 Murata T and Yamaguchi M (2014) Alternatively spliced variants of the regucalcin gene in various human normal and tumor tissues. *Int J Mol Med* **34**, 1141–1146.
  - 18 Yamaguchi M, Osuka S, Weitzmann MN, El-Rayes BF, Shoji M and Murata T (2016) Prolonged survival in pancreatic cancer patients with increased regucalcin gene expression: overexpression of regucalcin suppresses the proliferation in human pancreatic cancer MIA PaCa-2 cells *in vitro*. *Int J Oncol* **48**, 1955–1964.
  - 19 Yamaguchi M, Osuka S, Weitzmann MN, Shoji M and Murata T (2016) Increased regucalcin gene expression extends survival in breast cancer patients: overexpression of regucalcin suppresses the proliferation and metastatic bone activity in MDA-MB-231 human breast cancer cells *in vitro*. *Int J Oncol* **49**, 812–822.
  - 20 Yamaguchi M, Osuka S, Weitzmann MN, El-Rayes BF, Shoji M and Murata T (2016) Prolonged survival in hepatocarcinoma patients with increased regucalcin gene expression: HepG2 cell proliferation is suppressed by overexpression of regucalcin *in vitro*. *Int J Oncol* **49**, 1686–1694.
  - 21 Selkoe DJ (2001) Alzheimer's disease: genes, proteins, and therapy. *Physiol Rev* **81**, 741–766.
  - 22 Mattson MP (2004) Pathways towards and away from Alzheimer's disease. *Nature* **430**, 631–639.
  - 23 Karran E, Mercken M and De Strooper B (2011) The amyloid cascade hypothesis for Alzheimer's disease: an appraisal for the development of therapeutics. *Nat Rev Drug Discov* **10**, 698–712.
  - 24 Palop JJ and Mucke L (2010) Amyloid- $\beta$ -induced neuronal dysfunction in Alzheimer's disease: from synapses toward neural networks. *Nat Neurosci* **13**, 812–818.
  - 25 Bezprozvanny I and Mattson MP (2008) Neuronal calcium mishandling and the pathogenesis of Alzheimer's disease. *Trends Neurosci* **31**, 454–463.
  - 26 Magi S, Castaldo P, Macrì ML, Maiolino M, Matteucci A, Bastioli G, Gratteri S, Amoroso S and Lariccia V (2016) Intracellular calcium dysregulation: implications for Alzheimer's disease. *Biomed Res Int* **2016**, 6701324.
  - 27 Demuro A, Parker I and Stutzmann GE (2010) Calcium signaling and amyloid toxicity in Alzheimer disease. *J Biol Chem* **285**, 12463–12468.
  - 28 Demuro A and Parker I (2013) Cytotoxicity of intracellular A $\beta_{42}$  amyloid oligomers involves Ca $^{2+}$  release from the endoplasmic reticulum by stimulated production of inositol trisphosphate. *J Neurosci* **33**, 3824–3833.
  - 29 McKee AC, Kosik KS, Kennedy MB and Kowall NW (1990) Hippocampal neurons predisposed to neurofibrillary tangle formation are enriched in type II calcium/calmodulin-dependent protein kinase. *J Neuropathol Exp Neurol* **49**, 49–63.
  - 30 Yamamoto H, Hiragami Y, Murayama M, Ishizuka K, Kawahara M and Takashima A (2005) Phosphorylation of tau at serine 416 by Ca $^{2+}$ /calmodulin-dependent protein kinase II in neuronal soma in brain. *J Neurochem* **94**, 1438–1447.
  - 31 Veeranna Kaji T, Boland B, Odrliin T, Mohan P, Basavarajappa BS, Peterhoff C, Cataldo A, Rudnicki A, Amin N, Li BS *et al.* (2004) Calpain mediates calcium-induced activation of the Erk 1,2 MAPK pathway and cytoskeletal phosphorylation in neurons: relevance to Alzheimer's disease. *Am J Pathol* **165**, 795–805.
  - 32 Hamano T and Yamaguchi M (2001) Inhibitory role of regucalcin in the regulation of Ca $^{2+}$  dependent protein kinases activity in rat brain neurons. *J Neurol Sci* **183**, 33–38.
  - 33 Yamaguchi M and Nishina N (1995) Characterization of regucalcin effect on proteolytic activity in rat liver cytosol: relation to cysteinyl-proteases. *Mol Cell Biochem* **148**, 67–72.
  - 34 Baba T and Yamaguchi M (1999) Stimulatory effect of regucalcin on proteolytic activity in rat renal cortex cytosol: involvement of thiol proteases. *Mol Cell Biochem* **195**, 87–92.
  - 35 Yamaguchi M (2012) Role of regucalcin in brain calcium signaling: involvement in aging. *Integr Biol* **4**, 825–837.
  - 36 Reddy PH and Beal MF (2008) Amyloid  $\beta$ , mitochondrial dysfunction and synaptic damage: implications for cognitive decline in aging and Alzheimer's disease. *Trends Mol Med* **14**, 45–53.
  - 37 Reddy PH, Manczak M, Mao P, Calkins MJ, Reddy AP and Shirendeb U (2010) Amyloid- $\beta$  and mitochondria in aging and Alzheimer's disease: implications for synaptic damage and cognitive decline. *J Alzheimers Dis* **20**, S499–S512.
  - 38 Wang X, Wang W, Li L, Perry G, Lee HG and Zhu X (2014) Oxidative stress and mitochondrial dysfunction in Alzheimer's disease. *Biochim Biophys Acta* **1842**, 1240–1247.
  - 39 Huang X, Atwood CS, Hartshorn MA, Multhaup G, Goldstein LE, Scarpa RC, Cuajungco MP, Gray DN, Lim J, Moir RD *et al.* (1999) The A $\beta$  peptide of Alzheimer's disease directly produces hydrogen peroxide through metal ion reduction. *Biochemistry* **38**, 7609–7616.
  - 40 Butterfield DA, Reed T, Newman SF and Sultana R (2007) Roles of amyloid  $\beta$ -peptide-associated oxidative stress and brain protein modifications in the pathogenesis of Alzheimer's disease and mild cognitive impairment. *Free Radic Biol Med* **43**, 658–677.
  - 41 Kaminsky YG, Tikhonova LA and Kosenko EA (2015) Critical analysis of Alzheimer's amyloid-beta toxicity to mitochondria. *Front Biosci* **20**, 173–197.

- 42 Law A, Gauthier S and Quirion R (2001) Neuroprotective and neurorescuing effects of isoform-specific nitric oxide synthase inhibitors, nitric oxide scavenger, and antioxidant against beta-amyloid toxicity. *Br J Pharmacol* **133**, 1114–1124.
- 43 Ill-Raga G, Ramos-Fernández E, Guix FX, Tajés M, Bosch-Morató M, Palomer E, Godoy J, Belmar S, Cerpa W, Simpkins JW *et al.* (2010) Amyloid- $\beta$  peptide fibrils induce nitro-oxidative stress in neuronal cells. *J Alzheimers Dis* **22**, 641–652.
- 44 Malinski T (2007) Nitric oxide and nitroxidative stress in Alzheimer's disease. *J Alzheimers Dis* **11**, 207–218.
- 45 Mangialasche F, Polidori MC, Monastero R, Ercolani S, Camarda C, Cecchetti R and Mecocci P (2009) Biomarkers of oxidative and nitrosative damage in Alzheimer's disease and mild cognitive impairment. *Ageing Res Rev* **8**, 285–305.
- 46 Murata T, Tsuboi M, Hikita K and Kaneda N (2006) Protective effects of neurotrophic factors on tumor necrosis factor-related apoptosis-inducing ligand (TRAIL)-mediated apoptosis of murine adrenal chromaffin cell line tsAM5D. *J Biol Chem* **281**, 22503–22516.
- 47 Morais Cardoso S, Swerdlow RH and Oliveira CR (2002) Induction of cytochrome *c*-mediated apoptosis by amyloid  $\beta$  25-35 requires functional mitochondria. *Brain Res* **931**, 117–125.
- 48 Murphy MP (2009) How mitochondria produce reactive oxygen species. *Biochem J* **417**, 1–13.
- 49 Arun P, Aleti V, Parikh K, Manne V and Chilukuri N (2011) Senescence marker protein 30 (SMP30) expression in eukaryotic cells: existence of multiple species and membrane localization. *PLoS ONE* **6**, e16545.
- 50 Ishigami A, Kondo Y, Nanba R, Ohsawa T, Handa S, Kubo S, Akita M and Maruyama N (2004) SMP30 deficiency in mice causes an accumulation of neutral lipids and phospholipids in the liver and shortens the life span. *Biochem Biophys Res Commun* **315**, 575–580.
- 51 Correia S, Vaz CV, Silva AM, Cavaco JE and Socorro S (2017) Regucalcin counteracts tert-butyl hydroperoxide and cadmium-induced oxidative stress in rat testis. *J Appl Toxicol* **37**, 159–166.
- 52 Sato T, Seyama K, Sato Y, Mori H, Souma S, Akiyoshi T, Kodama Y, Mori T, Goto S, Takahashi K *et al.* (2006) Senescence marker protein-30 protects mice lungs from oxidative stress, aging, and smoking. *Am J Respir Crit Care Med* **174**, 530–537.
- 53 Son TG, Zou Y, Jung KJ, Yu BP, Ishigami A, Maruyama N and Lee J (2006) SMP30 deficiency causes increased oxidative stress in brain. *Mech Ageing Dev* **127**, 451–457.
- 54 Yamaguchi M and Isogai M (1993) Tissue concentration of calcium-binding protein regucalcin in rats by enzyme-linked immunoadsorbent assay. *Mol Cell Biochem* **122**, 65–68.
- 55 Puzzo D, Palmeri A and Arancio O (2006) Involvement of the nitric oxide pathway in synaptic dysfunction following amyloid elevation in Alzheimer's disease. *Rev Neurosci* **17**, 497–523.
- 56 Nakamura T and Lipton SA (2011) Redox modulation by S-nitrosylation contributes to protein misfolding, mitochondrial dynamics, and neuronal synaptic damage in neurodegenerative diseases. *Cell Death Differ* **18**, 1478–1486.
- 57 Bisaglia M, Venezia V, Piccioli P, Stanzione S, Porcile C, Russo C, Mancini F, Milanese C and Schettini G (2002) Acetaminophen protects hippocampal neurons and PC12 cultures from amyloid  $\beta$ -peptides induced oxidative stress and reduces NF- $\kappa$ B activation. *Neurochem Int* **41**, 43–54.
- 58 Keil U, Bonert A, Marques CA, Scherping I, Weyermann J, Strosznajder JB, Müller-Spahn F, Haass C, Czech C, Pradier L *et al.* (2004) Amyloid  $\beta$ -induced changes in nitric oxide production and mitochondrial activity lead to apoptosis. *J Biol Chem* **279**, 50310–50320.
- 59 Jang JH, Aruoma OI, Jen LS, Chung HY and Surh YJ (2004) Ergothioneine rescues PC12 cells from beta-amyloid-induced apoptotic death. *Free Radic Biol Med* **36**, 288–299.
- 60 Esposito G, De Filippis D, Maiuri MC, De Stefano D, Carnuccio R and Iuvone T (2006) Cannabidiol inhibits inducible nitric oxide synthase protein expression and nitric oxide production in  $\beta$ -amyloid stimulated PC12 neurons through p38 MAP kinase and NF- $\kappa$ B involvement. *Neurosci Lett* **399**, 91–95.
- 61 Yamaguchi M, Takakura Y and Nakagawa T (2008) Regucalcin increases Ca<sup>2+</sup>-ATPase activity in the mitochondria of brain tissues of normal and transgenic rats. *J Cell Biochem* **104**, 795–804.
- 62 Sun L, Wang L, Sun Y, Tang SW and Hu Y (2006) Protective effects of EUK4010 on  $\beta$ -amyloid(1-42) induced degeneration of neuronal cells. *Eur J Neurosci* **24**, 1011–1019.